

Stabilization of Biodiesel Fuel at Elevated Temperature with Hydrogen Donors: Evaluation with the Advanced Distillation Curve Method

Thomas J. Bruno,* Arron Wolk, and Alexander Naydich

Physical and Chemical Properties Division, National Institute of Standards and Technology,
Boulder, Colorado 80305

Received September 3, 2008. Revised Manuscript Received October 27, 2008

Recently, we introduced the concept of an advanced distillation curve measurement. The new metrology features several important aspects. First, we incorporate a composition explicit data channel for each distillate fraction (for both qualitative, quantitative, and trace analysis). The temperature, volume, and pressure measurements are of low uncertainty, and the temperatures are true thermodynamic state points that can be modeled with an equation of state. These two features make the measurements suitable for equation of state development. The approach also provides consistency with a century of historical data, an assessment of the energy content of each distillate fraction, and where needed, a corrosivity assessment of each distillate fraction. We have applied the new method to fundamental work with hydrocarbon mixtures and azeotropic mixtures, and also to real fuels. The fuels we have measured include rocket propellants, gasolines, jet fuels, diesel fuels (including oxygenated diesel fuel and biodiesel fuels), and crude oils. In this article, we show that the method can also be used to assess the combined thermal and oxidative stability of sensitive fluids such as biodiesel fuel. We also use the method to test three hydrogen donor molecules (1,2,3,4-tetrahydroquinoline (THQ), 1,2,3,4-tetrahydronaphthalene, and *trans*-decahydronaphthalene) for use as potential stabilizers for biodiesel fuel with this new method.

Introduction

Biodiesel Fuel. Biodiesel fuel has been the focus of a great deal of media attention and scientific research in the last several years as a potential replacement or extender for petroleum-derived diesel fuel.¹ The major constituents (fatty acid methyl esters, FAMES) of pure biodiesel are generally relatively few, consisting mainly of methyl palmitate, methyl stearate, methyl oleate, methyl linoleate, and methyl linolenate.² As a fuel for compression ignition engines, biodiesel fuel has several advantages, which include its renewability (biodiesel can be prepared from sources such as vegetable oil, animal fats, used cooking oil, and microalgae), the potential to produce it domestically, and increased lubricity compared to low-sulfur petroleum-derived diesel fuel fuels. The fluid is noncarcinogenic, nonmutagenic, and biodegradable, the use of which decreases certain emissions (including carbon monoxide, unburned hydrocarbon, and particulate matter). There are also some serious disadvantages to biodiesel fuel, including increased NO_x emissions, moisture absorption during storage, and chemical instability. The last item is especially problematic at higher temperatures.^{3–5}

The instability is of both an oxidative and a thermal nature, and of course they are related because the oxidation rate is faster at higher temperatures. Although these mechanisms are related, they generally occur in different process regimes. Oxidation typically occurs at lower temperatures, whereas thermal decomposition mechanisms occur at higher temperatures. For convenience in defining testing protocols however, many authors separate thermal and oxidative mechanisms and define thermal decomposition as that which occurs at high temperature (with the onset between 250 and 300 °C) in the absence of oxygen. On a practical level, there is no reason to separate the effects because the deleterious effects on engine operation are the result of both mechanisms. Indeed, the thermal effects on oxidative stability can be seen in modern engines in which fuel is recirculated.⁶ Moreover, there is interest in the application of fluids similar to B100 as aviation fuels, where such recirculation (and exposure to higher temperatures) is more common.

The oxidative instability begins immediately after production and occurs by a free radical chain reaction that will continue until the reactive molecular links (bis-allylic carbons) are depleted. Instability is also the result of the presence of double bonds (conjugated diene groups) on the FAME chains. Peroxides and hydroperoxides are reactive oxidizing agents that are formed during biodiesel fuel oxidation. The addition of antioxidants to retard the low temperature or storage oxidation of vegetable oils is a mature technology. Antioxidants classified as primary (chain breaking) or secondary (hydroperoxide decomposers)

* To whom correspondence should be addressed. E-mail: bruno@boulder.nist.gov.

(1) Knothe, G.; VanGerpen, J.; Krahl, J. *The Biodiesel Handbook*; American Oil Chemists' Association Press, Champaign, IL, 2005.

(2) Ott, L. S.; Huber, M. L.; Bruno, T. J. Density and Speed of Sound Measurements on Five Fatty Acid Methyl Esters at 83 kPa and Temperatures from (278.15 to 338.15) K. *J. Chem. Eng. Data* **2008**, *53*, 2412–2416.

(3) Characterization of Biodiesel Oxidation and Oxidation Products, CRC Project AVFL-2b, SWRI Project No. 08–10721. 2005.

(4) Paligova, J.; Jorikova, L.; Cveňgros, J. Study of FAME Stability. *Energy Fuels* **2008**, *22*, 1991–1996.

(5) Sarin, R.; Sharma, M.; Sinharay, S.; Malhotra, R. K. Jatropa Palm Biodiesel Blends: An Optimum Mix for Asia. *Fuel* **2007**, *86*, 1365–1371.

(6) Mittelbach, M.; Remschmidt, C. *Biodiesel: The Comprehensive Handbook*; Boersedruk: Graz, Austria, 2006.

have been used for approximately 80 years.⁷ Some of these are natural products (such as the tocopherols), whereas many of the sterically hindered phenols are synthetics. Some of the more effective synthetics are *t*-butylhydroquinone, pyrogallol, and propyl gallate, all of which are useful for slowing storage instability of biodiesel fuel.³ Typical antioxidant additive concentrations are 50 to 500 ppm (mass/mass).

Advanced Distillation Curve Metrology. In earlier work, we described a method and apparatus for an advanced distillation curve (ADC) measurement that is especially applicable to the characterization of fuels. This method is a significant improvement over current approaches. First, we incorporate a composition explicit data channel for each distillate fraction (for both qualitative, quantitative, and trace analysis). The temperature, volume, and pressure measurements are of low uncertainty, and the temperatures are true thermodynamic state points that can be modeled with an equation of state. These two features make the measurements suitable for equation of state development. The approach also provides consistency with a century of historical data, an assessment of the energy content of each distillate fraction, and where needed, a corrosivity assessment of each distillate fraction.^{8–14} The fuels we have measured include rocket propellants, gasolines, jet fuels, diesel fuels (including oxygenated diesel fuel and biodiesel fuels), and crude oils.^{15–24} For diesel fuels, the distillation curve is one of the

main operational and design parameters used to ensure good engine performance and optimization. The distillation curve can be correlated with mutagenicity of exhaust particulates, soot formation, cetane number, and of course it is critical in the development of models such as equations of state that are important in process development. Distillation data is also important in the optimization of processes that utilize distillation as a cleanup step. The measurement of petroleum-derived diesel fuels with this atmospheric pressure method requires heating the sample to approximately 325 °C, whereas the corresponding measurement of biodiesel fuels require a final temperature of approximately 385 °C.

In this article, we introduce another application of the ADC approach; the assessment of the combined oxidative and thermal stability of the fluid measured. We recognize that our work here on a particular B100 fluid is limited to this one fluid, and in this respect this report must be considered preliminary. We further recognize that there are many variations of B100; indeed we have produced and tested our own such fluid made from olive oil. Here, we have chosen as a demonstration of the technique a commercially available soy based B100 that is considered typical.

In addition to the metrology demonstration, we use this method to demonstrate the efficacy of three hydrogen donor additives in decreasing the oxidative decomposition of biodiesel fuel. In this respect, the ADC can be used as an accelerated stability test.

Hydrogen Donors. Much of the literature on hydrogen donor fluids comes from coal liquefaction processes.²⁵ Hydrogen donors are fluids or solvents that are capable of providing hydrogen to enable the conversion of heavier residuals into distillable fractions. Moreover, they have been used to prevent the formation of coke deposits by the heavier residuals.^{26,27} They serve the added purpose of a solvent, capable of dissolving heavy aromatic compounds. The classical donor solvent is composed of a saturated ring attached to an aromatic ring.^{28,29} In coal liquefaction processes, coal is converted in such a solvent at temperatures between 400 and 475 °C. Ideally, industrial solvents used in such processes should be recyclable, or at least inexpensive. Typically, hydrogen donor solvents have been added externally from petroleum residuals or anthracene oils (that is, byproduct from other processes), thus making them favorable candidates.

The hydrogen donor capability of many of these fluids has been exploited in the stabilization of aviation fuels. The literature

(7) McCormick, R. L.; Westbrook, S. R., *Empirical Study of the Stability of Biodiesel and Biodiesel Blends*; Milestone Report NREL/TP-540-41619; National Renewable Energy Laboratory: United States Department of Energy, 2007.

(8) Bruno, T. J. Improvements in the measurement of distillation curves - part 1: a composition-explicit approach. *Ind. Eng. Chem. Res.* **2006**, *45*, 4371–4380.

(9) Bruno, T. J.; Smith, B. L. Improvements in the Measurement of Distillation Curves—Part 2: Application to Aerospace/Aviation Fuels RP-1 and S-8. *Ind. Eng. Chem. Res.* **2006**, *45*, 4381–4388.

(10) Bruno, T. J. Method and Apparatus for Precision In-Line Sampling of Distillate. *Sep. Sci. Technol.* **2006**, *41* (2), 309–314.

(11) Bruno, T. J.; Smith, B. L. Enthalpy of Combustion of Fuels as a Function of Distillate Cut: Application of an Advanced Distillation Curve Method. *Energy Fuels* **2006**, *20*, 2109–2116.

(12) Smith, B. L.; Bruno, T. J. Improvements in the Measurement of Distillation Curves: Part 3—Application to Gasoline and Gasoline + Methanol Mixtures. *Ind. Eng. Chem. Res.* **2006**, *46*, 297–309.

(13) Smith, B. L.; Bruno, T. J. Improvements in the Measurement of Distillation Curves: Part 4—Application to the Aviation Turbine Fuel Jet-A. *Ind. Eng. Chem. Res.* **2006**, *46*, 310–320.

(14) Smith, B. L.; Bruno, T. J. Advanced Distillation Curve Measurement with a Model Predictive Temperature Controller. *Int. J. Thermophys.* **2006**, *27*, 1419–1434.

(15) Bruno, T. J. *The Properties of S-8*; Final Report for MIPR F4FBEY6237G001; Air Force Research Laboratory, 2006.

(16) Bruno, T. J.; Laescke, A.; Outcalt, S. L.; Seelig, H.-D.; Smith, B. L. Properties of a 50/50 Mixture of Jet-A + S-8, NIST-IR-6647, 2007.

(17) Ott, L. S.; Bruno, T. J. Variability of Biodiesel Fuel and Comparison to Petroleum-Derived Diesel Fuel: Application of a Composition and Enthalpy Explicit Distillation Curve Method. *Energy Fuels* **2008**, *22*, 2861–2868.

(18) Ott, L. S.; Bruno, T. J. Corrosivity of Fluids as a Function of Distillate Cut: Application of an Advanced Distillation Curve Method. *Energy Fuels* **2007**, *21*, 2778–2784.

(19) Ott, L. S.; Smith, B. L.; Bruno, T. J. Advanced Distillation Curve Measurements for Corrosive Fluids: Application to Two Crude Oils. *Fuel* **2008**, *87*, 3055–3064.

(20) Ott, L. S.; Smith, B. L.; Bruno, T. J. Advanced Distillation Curve Measurement: Application to a Bio-Derived Crude Oil Prepared from Swine Manure. *Fuel* **2008**, *87*, 3379–3387.

(21) Ott, L. S.; Smith, B. L.; Bruno, T. J. Composition-Explicit Distillation Curves of Mixtures of Diesel Fuel with Biomass-Derived Glycol Ester Oxygenates: A Fuel Design Tool for Decreased Particulate Emissions. *Energy Fuels* **2008**, *22*, 2518–2526.

(22) Smith, B. L.; Ott, L. S.; Bruno, T. J. Composition-Explicit Distillation Curves of Diesel Fuel with Glycol Ether and Glycol Ester Oxygenates: A Design Tool for Decreased Particulate Emissions. *Environ. Sci. Technol.* **2008**, *42*, 7682–7689.

(23) Smith, B. L.; Bruno, T. J. Application of a Composition-Explicit Distillation Curve Metrology to Mixtures of Jet-A + Synthetic Fischer-Tropsch S-8. *J. Propul. Power* **2008**, *24* (3), 619–623.

(24) Smith, B. L.; Ott, L. S.; Bruno, T. J. Composition-Explicit Distillation Curves of Commercial Biodiesel Fuels: Comparison of Petroleum Derived Fuel with B20 and B100. *Ind. Eng. Chem. Res.* **2008**, *47* (16), 5832–5840.

(25) Burgess, C.; Schobert, H. Behavior of Tetrahydroquinoline in Temperature Staged Liquefaction of Subbituminous Coal. *Fuel* **1991**, *70*, 372–379.

(26) Coleman, M.; Selvaraj, M.; Sobkowiak, M.; Yoon, E. Potential Stabilizers for Jet Fuels Subjected to Thermal Stress above 400 °C. *Energy Fuels* **1992**, *6*, pp 535–539.

(27) Corporan, E.; Minus, D. K. Assessment of Radical Stabilizing Additives for JP-8. 34th AIAA/ASME/SAE/ASEE Joint Propulsion Conference and Exhibit, July 13–15, 1998, Cleveland, OH, AIAA 98–3996.1998.

(28) Yoon, E.; Selvaraj, L.; Eser, S.; Coleman, M. High Temperature Stabilizers for Jet Fuels and Similar Hydrocarbon Mixtures. 2. Kinetic Studies. *Energy Fuels* **1996**, *10*, 812–815.

(29) Yoon, E.; Selvaraj, L.; Eser, S.; Coleman, M. High Temperature Stabilizers for Jet Fuels and Similar Hydrocarbon Mixtures 1. Comparative Studies of Hydrogen Donors. *Energy Fuels* **1996**, *10*, 806–811.

(as well as our own studies³⁰) indicates that fluids such as 1,2,3,4-tetrahydroquinoline (THQ), 1,2,3,4-tetrahydronaphthalene, and *trans*-decahydronaphthalene are suitable fluids to consider for fuel stabilization.²⁷ Hydrogen donors act to cap aliphatic radicals formed at temperatures in excess of 300 °C (the limit discussed earlier). In so doing, C2 and C3 alkyl aromatic compounds are typically formed. Most of the studies done with hydrogen donors to stabilize aviation fuels employ relatively large concentrations of additive, up to 5% (mass/mass).^{26,27} Some authors will refer to antioxidants added in the 50 to 500 ppm (mass/mass) range as additives and those components added in the percent range as stabilizers. We use the terms interchangeably. Clearly, however, for performance and economic reasons, it is desirable to minimize the concentrations where possible.

Experimental Section

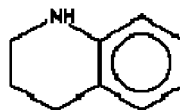
The *n*-hexane used as a solvent in this work was obtained from a commercial supplier and was analyzed by gas chromatography (30 m capillary column of 5% phenyl/95% dimethyl polysiloxane having a thickness of 1 μm , temperature program from 50 to 170 °C, 5 °C per minute) using flame ionization detection and mass spectrometric detection.^{31,32} These analyses revealed the purity to be approximately 99.9%, and the fluid was used without further purification.

The biodiesel fuel used in this work was B100 obtained from a commercial supplier and was used without modification. It was manufactured from a soy feedstock and met or exceeded all aspects of the applicable fuel specification.³³ This sample was analyzed by gas chromatography with flame ionization detection on a 30 m capillary column with a 0.1 mm coating of 50% cyanopropyl/50% dimethylpolysiloxane as the stationary phase. This phase provides separations based upon polarity and is specifically intended for the analysis of the FAMES that compose biodiesel fuel. Samples were injected via syringe into a split/splitless injector set with a 50 to 1 split ratio. The injector was operated at a temperature of 325 °C and a constant head pressure of 10 psig. The sample residence time in the injector was very short, thus the effect of sample exposure to this high temperature is expected to be minimal. The column was temperature programmed to provide complete and rapid elution with minimal loss of peak shape. Initially, the temperature was maintained isothermally at 80 °C for 2 min, followed by a 8 °C/min ramp to 285 °C, and finally maintained at 285 °C for 5 min. Although the analysis was allowed to run for more than 33 min, all peaks were eluted after approximately 19 min. Previous measurements of the distillation curve of this fluid as well as several other biodiesel fuels showed that the B100 we used here is representative in terms of the thermophysical and chemical properties of biodiesel fuel.

The hydrogen donor additives used in this work were 1,2,3,4-tetrahydroquinoline (THQ, CAS No. 635-46-1), 1,2,3,4-tetrahydronaphthalene (tetralin, CAS No: 119-64-2), and *trans*-decahydronaphthalene (*t*-decalin, CAS No: 119-64-2). Some representative properties for these materials are provided in Table 1.³⁴ These fluids were obtained from a commercial source with specified purities of

Table 1. Information on the Hydrogen Donor Compounds Studied in This Work

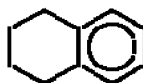
1,2,3,4-tetrahydroquinoline:



CAS No. 635-46-1
InChI=1/C9H11N/c1-2-6-9-8(4-1)5-3-7-10-9/h1-2,4,6,10H,3,5,7H2

RMM = 133.19
T_{boil} = 249 °C
T_{fus} = 10-15 °C
Density = 1.061 g/mL (20 °C)
Refractive Index, n_D²⁰ = 1.593 (25 °C)
Synonyms: Kusol; 1,2,3,4-tetrahydroquinoline; tetrahydroquinoline; 1,2,3,4-tetrahydroquinoline.

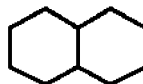
1,2,3,4-tetrahydronaphthalene:



CAS No: 119-64-2
InChI=1/C10H12/c1-2-6-10-8-4-3-7-9(10)5-1/h1-2,5-6H,3-4,7-8H2

RMM = 132.2
T_{boil} = 207 °C
T_{fus} = -35 °C
Density = 0.970 g/mL (20 °C)
Refractive Index, n_D²⁰ = 1.5410 - 1.5411 (25 °C)
Synonyms: naphthalene, 1,2,3,4-tetrahydro-; benzocyclohexane; tetrahydronaphthalene; tetralin; tetraline; tetranap; 1,2,3,4-tetrahydronaphthalene; naphthalene-1,2,3,4-tetrahydride; δ 5,7,9-naphthantriene; bacticin; tetralina; tetralene.

trans-decahydronaphthalene:



CAS No: 91-17-8
InChI=1/C10H18/c1-2-6-10-8-4-3-7-9(10)5-1/h9-10H,1-8H2

RMM = 138.2
T_{boil} = 187 °C
T_{fus} = -31 °C
Density = 0.896 g/mL (20 °C)
Refractive Index, n_D²⁰ = 1.469 - 1.481 (25 °C)
Synonyms: bicyclo[4.4.0]decane; dec; decahydronaphthalene; *t*-decalin; decalin; dekalin; naphthan; perhydronaphthalene; decanhydronaphthalene; dekalina; naphthalene; naphthane; decaline.

between 97 and 99% (mass/mass). The purity of each of the additives was verified by gas chromatography (30 m capillary column of 5% phenyl/95% dimethyl polysiloxane having a thickness of 1 μm , temperature program from 50 to 170 °C, 5 °C per minute) using flame ionization detection and mass spectrometric detection. These analyses revealed the purity to be better than the specifications (no fluid had a purity of less than 99% on the basis of raw area counts), and the fluids were used without further purification. Mixtures of B100 with 1 and 3% (v/v) of the hydrogen donor liquids listed in Table 1 were prepared in mixing cylinders just prior to measurement. Solutions were kept in capped containers to minimize evaporation of any volatiles and also to minimize the uptake of moisture.

The method and apparatus for the advanced distillation curve measurement has been reviewed in a number of sources summarized earlier, so additional general description will not be provided here. Rather, we will focus only on the modifications that were required for the study of biodiesel fuel.

We found in earlier work on B100 that the thermal and oxidative instability of this fluid prevented the measurement of a distillation curve with our usual ADC approach.²⁴ Discrepancies in temperature of up to 20 °C were observed between successive distillation curve measurements. We found that the addition of an inert gas sparge incorporated into the distillation flask eliminated the problem and allowed the measurement of highly reproducible distillation curves.

(30) Widegren, J. A.; Bruno, T. J. The Properties of RP-1 and RP-2, Interim Report, MIPR FISBAA8022G001; March, 2008.

(31) Bruno, T. J.; Svoronos, P. D. N. *CRC Handbook of Basic Tables for Chemical Analysis*, 2nd. ed.; Taylor and Francis CRC Press: Boca Raton, 2004.

(32) Bruno, T. J.; Svoronos, P. D. N. *CRC Handbook of Fundamental Spectroscopic Correlation Charts*; Taylor and Francis CRC Press: Boca Raton, 2005.

(33) Standard Specification for Biodiesel Fuel Blend Stock (B100) for Middle Distillate Fuels, ASTM Standard D-6751-08, Book of Standards Volume 05-04, 2008.

(34) Linstrom, P. J.; Mallard, W. G., *NIST Chemistry WebBook, NIST Standard Reference Database Number 69*; National Institute of Standards and Technology: Gaithersburg MD, 20899 (<http://webbook.nist.gov>), June 2005.

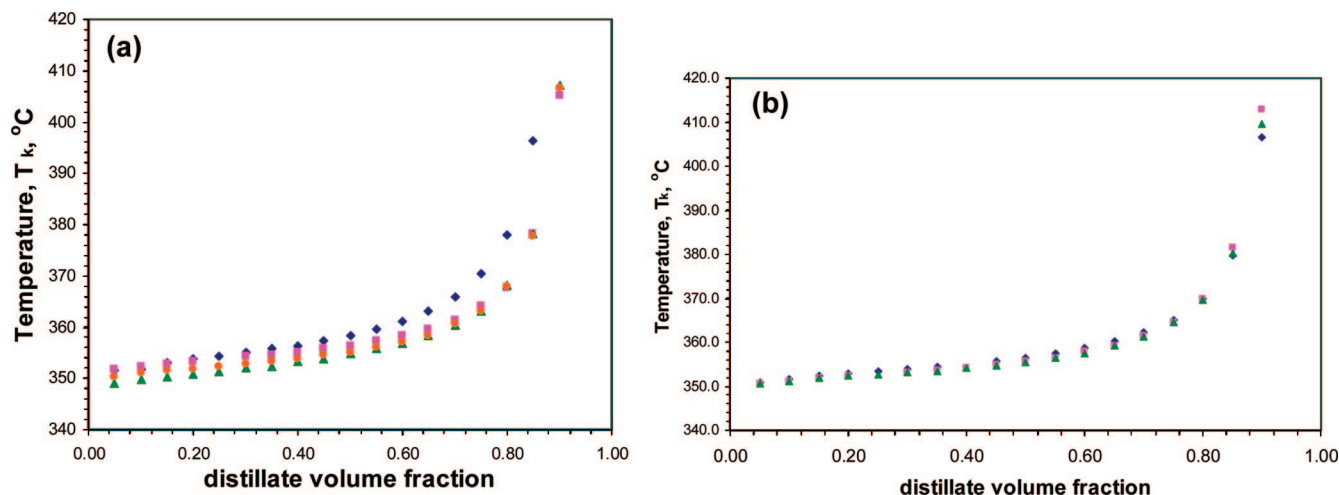


Figure 1. a: Representative distillation curves of B100 measured without an inert gas sparge. The spread in the measured temperatures of each curve ranges from 3 to 20 °C, with an average standard deviation of 2.8 °C. b: Representative distillation curves of B100 measured with the inert gas sparge. The spread (range) in the measured temperatures of each curve ranges from 0.3 to 1.7 °C, with an average standard deviation of 0.4 °C.

The sparge was provided by a stainless steel capillary tubing having an inside diameter of 0.23 mm that entered the top of the flask in the same feed-through used for the thermocouples. Because it is possible to quantitatively assess the tightening of the distillation curve measurement upon the addition of the sparge, we can use this change as a means of assessing the oxidative stability of the fluids being measured. We demonstrate this procedure here with distillation curves measured for B100 with and without an inert gas sparge.

The inert gas sparge described above was used to bubble an inert gas blanket into the distillation flask prior to measurement and then provide a very gentle flow of inert gas into the flask during the measurement. We have used high-purity nitrogen gas as the blanket in early measurements but found that high-purity argon, with its higher molecular mass and viscosity, was a better choice. For the premeasurement sparge, the stainless steel capillary was submerged in the fluid, and the gas flooding (at approximately 50 mL/min) was allowed to continue for 5 min. During the measurement, the capillary was lifted out of the fluid to a position of approximately 5 cm above the surface of the liquid, and the flow rate was reduced to approximately 1 mL/min. The sparge was used only for the comparative measurements on B100 without any additive.

The measurements performed on B100 with hydrogen donor additives were all done without the inert gas sparge. No provision was made to exclude air from the distillation flask. For these measurements, 1% and 3% (v/v) solutions of B100 with the hydrogen donors were prepared in mixing cylinders and then stored at ambient temperature in sealed vessels until the measurement was completed. In no case was the storage time more than two hours.

The required fluid for the distillation curve measurement (in each case 200 mL) was placed into the boiling flask with a 200 mL volumetric pipet. The thermocouples were then inserted into the proper locations to monitor T_k , the temperature in the fluid and T_h , the temperature at the bottom of the takeoff position in the distillation head. Enclosure heating was then commenced with a four-step program based upon a previously measured distillation curve. Volume measurements were made in the level-stabilized receiver, and sample aliquots were collected at the receiver adapter hammock. In the course of this work, we performed between four and six complete distillation curve measurements for each of the fluid samples.

Because the measurements of the distillation curves were performed at ambient atmospheric pressure (typically 83 kPa, measured with an electronic barometer), temperature readings were corrected for what should be obtained at standard atmospheric pressure. This was done with the modified Sydney Young equation, in which the constant term was assigned a value of 0.000097.^{35–38} This value corresponds to an *n*-alkane carbon chain of 17. With

biodiesel, we also have polar ester groups on the chains. A polar moiety such as this can be expected to slightly lower the constant term, although no data are available on fluids such as FAMES to verify this. Moreover, because the oleate group is typically one moiety on a long hydrocarbon chain (that may contain 16–18 carbons), the change that may potentially be introduced into this constant term will likely be negligible. We make no adjustment to the constant for the addition of the hydrogen donor additives, and we expect that the uncertainty so introduced will be negligible. In previous work, we have treated in detail the other sources of uncertainty in the application of the Sydney Young equation.³⁵

Results and Discussion

1. Distillation Curve as a Measure of Oxidative Stability.

To demonstrate the application of the ADC method to assess the oxidative stability of biodiesel fuel (and by extension, any oxidative unstable or sensitive fluid), we have measured several distillation curves of the same batch of a representative B100 fluid, with and without the inert gas sparge as described in the experimental section. In part a of Figure 1, we present four distillation curves for B100 measured without the inert gas. We note by examining the figure that the absolute temperature range or discrepancy between the measured curves ranges from 3 to 20 °C, clearly worsening at higher temperatures as the effects of thermal decomposition and oxidation increase. In this context, we use the term absolute to indicate the full range rather than an average. This level of distillation curve repeatability late in the curve is unacceptable as a measure of fuel volatility specification. Indeed, many diesel engine operating parameters (for example, ignition delay and the mutagenicity of the exhaust) are correlated with the response in this region of the curve.³⁹ Moreover, such a series of results could not even be considered for more sophisticated applications such as modeling or equation

(35) Ott, L. S.; Smith, B. L.; Bruno, T. J. Experimental Test of the Sydney Young Equation for the Presentation of Distillation Curves. *J. Chem. Thermodyn.* **2008**, *40*, 1352–1357.

(36) Young, S. Correction of Boiling Points of Liquids from Observed to Normal Pressures. *Proc. Chem. Soc.* **1902**, *81*, 777.

(37) Young, S. *Fractional Distillation*; Macmillan and Co., Ltd.: London, 1903.

(38) Young, S. *Distillation Principles and Processes*; Macmillan and Co., Ltd.: London, 1922.

(39) Sjoren, M.; Li, H.; Banner, C.; Raftner, J.; Westerholm, R.; Rannug, U. Influence of Physical and Chemical Characteristics of Diesel Fuels and Exhaust Emissions on Biological Effects of Particle Extracts. *Chem. Res. Toxicol.* **1996**, *9*, 197–207.

of state development.^{40,41} Ideally, replicate measurements of the distillation curve should overlay, and in previous work we have shown that a curve-to-curve repeatability of 0.5 °C is possible. We note that our claimed experimental uncertainty for the ADC is less than this, listed at 0.2 °C. The repeatability from curve to curve is a different circumstance, however, because it also dependent upon the adjustment of the Sydney Young equation and the variation in the measured atmospheric pressure.

If we measure the distillation curves with the inert gas sparge, the results shown in part b of Figure 1 are obtained. We note that now the results are far more repeatable. The absolute range of temperatures is now between 0.3 and 1.7 °C. Such a result is excellent for a fluid specification and entirely adequate for modeling and equation of state development. Indeed, the influence of atmospheric pressure variations on the Sydney Young adjustment can be eliminated by using the calibrated temperature and pressure results directly, and any modeling studies would be done in exactly that way. The observation that the exclusion of air from the distillation flask before and during measurement can result in such an improvement indicates that the difficulty manifest in part a of Figure 1 is primarily oxidative decomposition.

We can quantify the effect of oxidative decomposition by reducing to a numerical indicator the spread in the curves of Figure 1. Because we have multiple distillation curves to compare, for each distillate fraction (the x axes) in Figure 1, we can calculate the temperature range across distillate fraction for several curves as a measure of dispersion. Moreover, if we assume that the successive measurements of distillation curves are normally distributed, we can also calculate the standard deviation of the mean temperature. This is a valid assumption because each distillation curve is an independent event, each sample is treated exactly the same way, and there is no hysteresis among successive samples. Thus, we can calculate the dispersion in all of the temperature measurements for all curves at, for example, the 20% distillate fraction (0.20 on the x axes of parts a and b of of Figure 1). As an overall measure of dispersion over the entire distillate, we can calculate the average of each range and standard deviation, taken over each of the measured distillate fractions. This can be done for the entire curve and also for parts of the curve individually. Thus, we can measure the dispersion of the first and second halves of each curve.

In addition to these measures of dispersion, we can calculate the area subtended by the distillation curves. The areas between the curves with the highest and lowest kettle temperatures (at each distillate fraction) were found by first subtracting the average minimum temperature from the average maximum temperature for each pair of successive measurements. This value was then multiplied by the difference in distillate volume between each fraction (a constant 10 mL), giving a trapezoidal area for each pair of measurements. Whereas the area measurements are useful as qualitative or conceptual descriptors, they are correlated; the area of the entire curve is the sum of that of the first and second halves. This renders this measure somewhat less valuable as a statistical indicator of change; rather, it is a more visual indicator of dispersion. Moreover, the unit of this area is unusual (°C· δV , degrees multiplied by a volume fraction change). We therefore consider the average standard deviation

Table 2. Summary of the Average Temperature Ranges and Standard Deviations, and the Areas Subtended in Successive Distillation Curves, with and without the Use of an Inert Gas Sparge^a

	without sparge	with sparge	offset decrease ratio
entire distillation curve, 0–90%			
average range, °C	5.8	1.1	5.3
average std. dev., °C	2.8	0.4	7.0
area	1352	160	8.5
first half, 0–50%			
average range, °C	3.1	0.6	5.2
average std. dev., °C	1.4	0.3	4.7
area	259	51	5.1
second half, 50–90%			
average range, °C	7.7	1.0	7.1
average std. dev., °C	3.7	0.5	7.4
area	1094	109	10

^a The result for the full distillation curves, and also separately for the first and second halves, are provided. The average standard deviations, our favored measures of dispersion, are highlighted.

to be the most useful measure of dispersion, and therefore we highlight this value in the tables that follow.

In Table 2, we present the results of the data examination described above. For measurements made with and without the inert gas sparge, we list the average range, average standard deviation, and area subtended by the curves for the entire volume fraction range. We also list these values separately for the first and second halves of each curve. In the column on the right-hand side of the table, we provide the ration of each dispersion measure, with and without the sparge, as a means of comparison. This provides an overall numerical description of (1) the efficacy of the inert gas sparge, and (2) the oxidative decomposition occurring in the measurements performed without the sparge.

Considering first the measurements made on B100 without the sparge, we see that, for the entire distillate fraction range, the average range and standard deviation of the temperature are 5.8 and 2.8 °C, respectively. As we noted earlier, individual curve-to-curve discrepancies can be as high as 20 °C; working with the overall average simply provides a more convenient treatment. The total area subtended by the set of curves is 1352 (in essentially arbitrary units of °C· δV). Early in the distillations (from 0 to 50% in distillate fraction), these measures are lower at 3.1 and 1.4 °C, respectively but then later (from 50 to 90% in distillate fraction) this increases to 7.7 and 3.7 °C. We note the same trend with the area. This poor repeatability renders such measurements essentially useless for anything but the crudest applications. Upon application of the inert gas sparge, we note that the repeatability has improved dramatically. For the entire distillate fraction range, the average temperature spread is now 1.1 °C, the average standard deviation is 0.4 °C, and the total subtended area has decreased to 160. Early in the sparged distillations (from 0 to 50% in distillate fraction), we note an average range of 0.6 °C and an average standard deviation of 0.3 °C, whereas later in the distillations (from 50 to 90% in distillate fraction) this increases slightly to 1.0 and 0.5 °C, respectively. This repeatability is typical of what we have measured for highly stable fluids such as petroleum diesel fuels and is acceptable for all applications of the ADC.

The use of an inert gas sparge causes no anomalies in distillation curve measurement with low-volatility fluids such as biodiesel fuel, nor does it cause the loss of any volatile species. The air-cooled condenser prevents the loss of any volatiles and ensures that the components of all fractions are captured for analysis. This was demonstrated in earlier work in

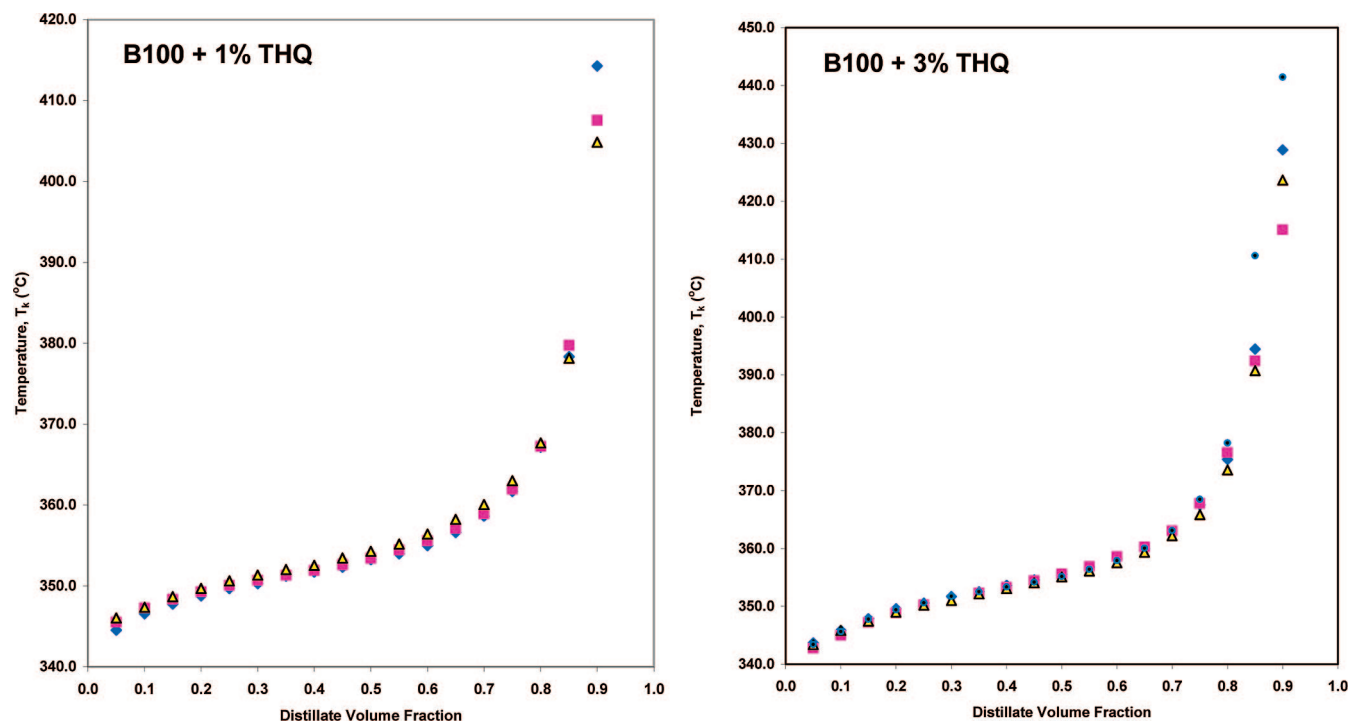
(40) Huber, M. L.; Smith, B. L.; Ott, L. S.; Bruno, T. J. Surrogate Mixture Model for the Thermophysical Properties of Synthetic Aviation Fuel S-8: Explicit Application of the Advanced Distillation Curve. *Energy Fuels* **2008**, *22*, 1104–1114.

(41) Huber, M. L.; Lemmon, E.; Diky, V.; Smith, B. L.; Bruno, T. J. Chemically Authentic Surrogate Mixture Model for the Thermophysical Properties of a Coal-Derived-Liquid Fuel. *Energy Fuels* **2008**, *22*, 3249–3257.

Table 3. Summary of the Average Temperature Ranges and Standard Deviations and the Areas Subtended in Successive Distillation Curves Measured with 1 and 3% of Added Hydrogen Donor Species^a

	1% (v/v)			3% (v/v)		
	avg. range, °C	avg. std. deviation, °C	area	avg. range, °C	avg. std. deviation, °C	area
			THQ			
full	1.6	0.8	230	1.8	0.9	497
0–50%	1.0	0.5	81	0.6	0.3	52
50–90%	1.3	0.7	149	1.6	0.8	445
			tetralin			
full	2.9	1.5	446	2.6	1.4	430
0–50%	1.0	0.5	82	0.4	0.2	37
50–90%	4.8	2.5	364	4.8	2.5	393
			<i>t</i> -decalin			
full	1.8	0.9	253	1.0	0.5	131
0–50%	0.3	0.2	24	0.3	0.2	27
50–90%	3.2	0.7	230	1.6	0.9	104

^a The result for the full distillation curves, and also separately for the first and second halves, are provided. The average standard deviations, our favored measures of dispersion, are highlighted.

**Figure 2.** Distillation curves for B100 with 1 and 3% THQ.

which a sample of B100 fuel obtained commercially was found to be slightly contaminated with some petroleum diesel fuel. This was likely the result of filling an existing diesel fuel tank with biodiesel fuel without first thoroughly cleaning the tank. We were easily able to capture and identify the lighter petroleum diesel fuel components in the earliest stage of the distillation curve. On the basis of the discussion above, we conclude that the inert gas sparge provides a benchmark for comparison of curve-to-curve reproducibility of sensitive fluids. We also conclude that measurements performed with and without the sparge provide a basis of assessing oxidative decomposition in an approximate fashion.

Stabilized Biodiesel Fuel-Distillation Curve Information.

Three replicate distillation curves were measured for each mixture of B100 with the additives and without the inert gas sparge. These measurements were designed to assess the effect of the hydrogen donor on retarding oxidative decomposition, as measured by the ADC curve-to-curve repeatability demonstrated above.

Following the presentation of the pure B100 measurements in Table 2, we provide the spread in successive distillation curve

measurements for B100 with 1 and 3% 1,2,3,4-tetrahydroquinoline (THQ), tetralin, and *t*-decalin in Table 3. The results are shown graphically in Figures 2, 3, and 4, respectively. We see that the addition of each of these additives makes a significant difference in the repeatability of the distillation curve. For the mixtures with 1% additive, the most effective of the three hydrogen donors is THQ, which nearly provides the stabilization effect obtained with the inert gas sparge. For example, the solution of B100 with 1% (v/v) THQ results in an average standard deviation in temperature of 0.8, whereas that with the sparge is 0.6 °C. The *t*-decalin performs nearly as well as THQ, and the relative performance of the additives we have studied is in the order: THQ > *t*-decalin ≫ tetralin. The observation that THQ performs the best as a hydrogen donor is similar to the observations of other researchers involved with formulation of high-temperature aviation fuels, albeit with different techniques. This observation is also in line with our own measurements in a series of thermal decomposition kinetics measurements on the stabilization of the rocket propellant RP-2 with some of these same additives (THQ and tetralin). There we measured global pseudofirst order decomposition rate constants

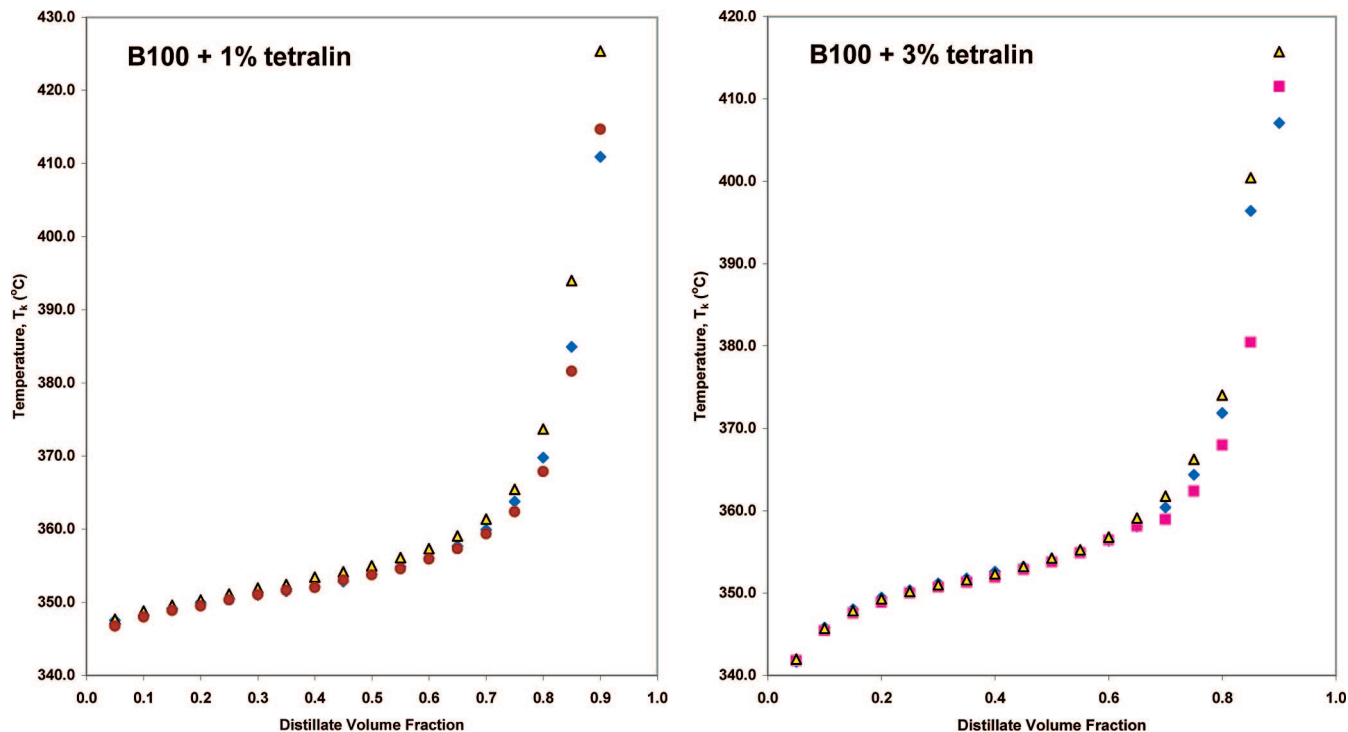


Figure 3. Distillation curves for B100 with 1 and 3% tetralin.

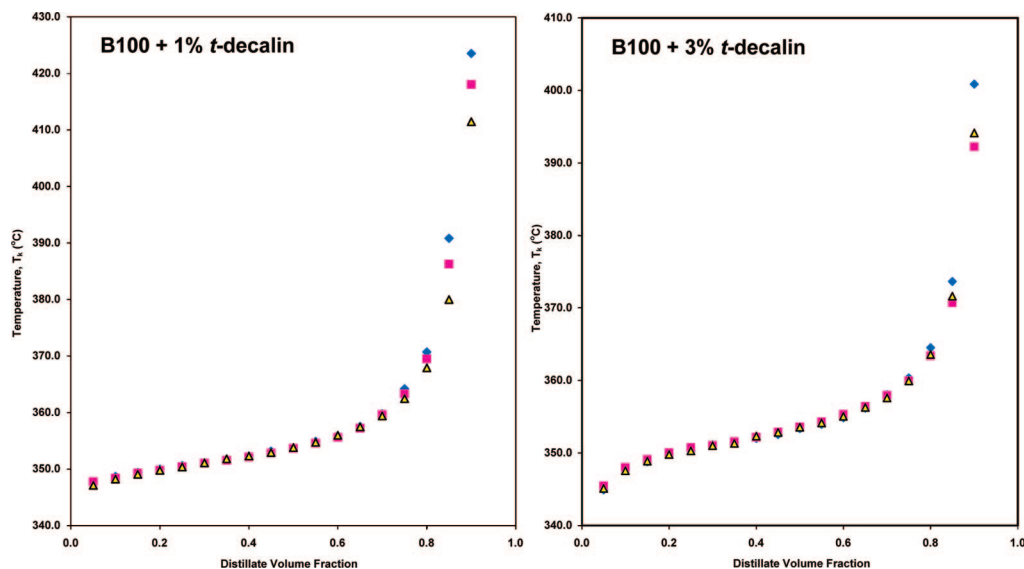


Figure 4. Distillation curves for B100 with 1 and 3% *t*-decalin.

by an ampule reactor technique, and the same trend in stabilization was noted.⁴²

In all of these measurements, the performance of the hydrogen donor additives is best at the lower temperatures, decreasing in effectiveness at higher temperatures as the additives react and themselves decompose. This was also noted in the kinetics study mentioned above. Increasing the additive concentration to 3% makes surprisingly little difference with THQ and tetralin, whereas the concentration enhancement with *t*-decalin is slightly higher.

In Table 3, we also present the stabilization effect split roughly in half, between the 0–50% and the 50–90% distillate fractions. Because distillation is a separation process, we would

expect the relatively volatile additives to have more of an effect in the early part of each curve. Moreover, the additives are depleted by their own decomposition into alkyl aromatics as the temperature increases later in the distillation. This effectively divides the performance of the additives into low- and high-temperature regions. We see that the additives in fact are always more effective early in the curve, before they distill out. It is interesting to note that, in our kinetics measurements on stabilized RP-2, we have concluded that the additives are more effective hydrogen donors at lower temperatures (below approximately 375 °C).

We note that *t*-decalin performs better than THQ in the early part of the distillations, but later THQ performs better. There are two reasons for this. First, *t*-decalin has the lowest boiling temperature of any of the hydrogen donors studied; thus, it will be distilled out of the biodiesel fluids relatively quickly. Second,

(42) Widgren, J. A.; Bruno, T. J. Thermal Decomposition Kinetics of the Kerosene Based Rocket Propellant RP-2 Stabilized with Three Additives. *Ind. Eng. Chem. Res.* 2008, submitted.

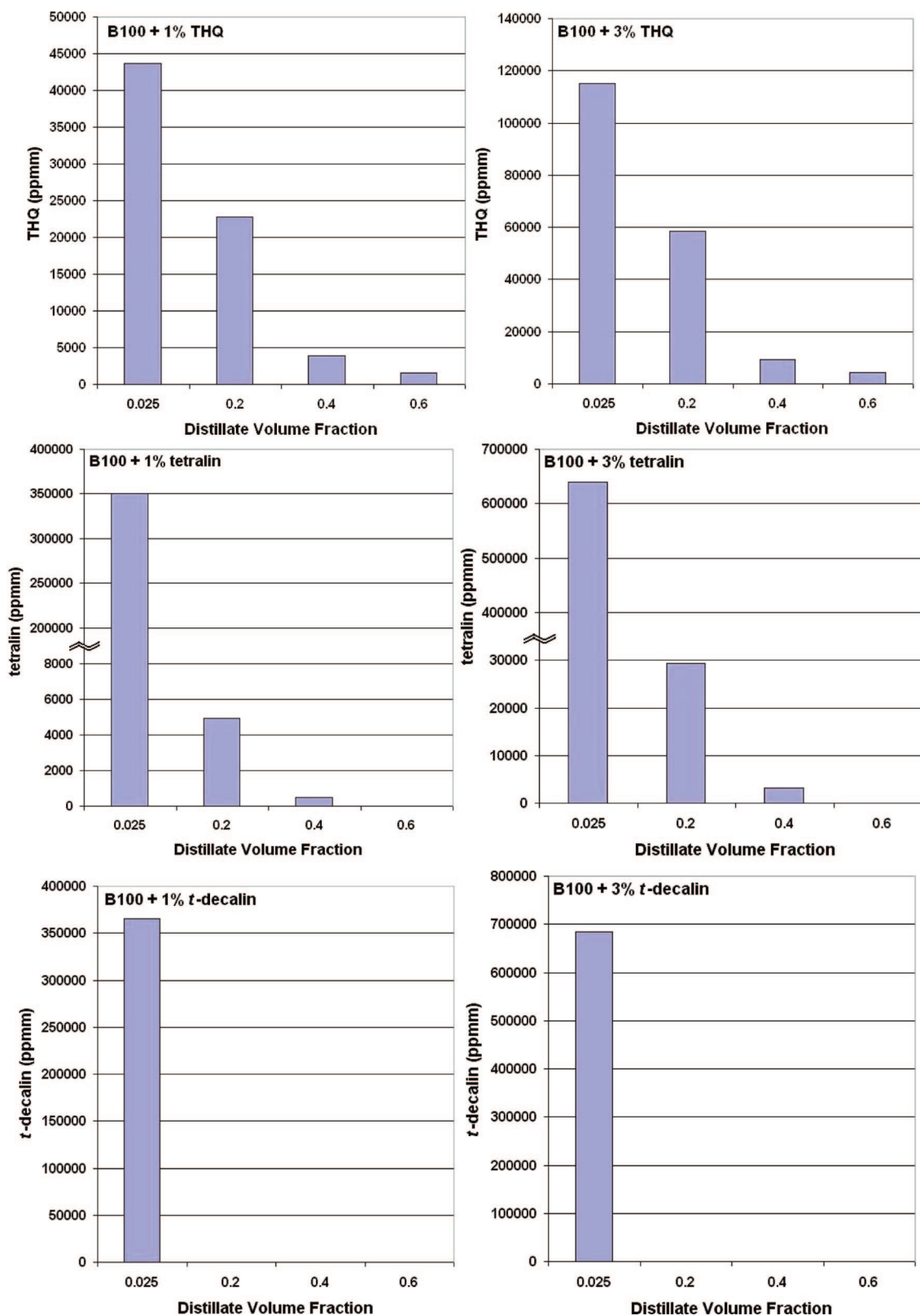


Figure 5. Histograms showing the concentrations of hydrogen donor (ppm, mass/mass) in selected distillate fractions. The uncertainty is discussed in the text.

t-decalin appears to be consumed faster in kinetic studies. In an evaluation of hydrogen donor fluids in a surrogate aviation fuel, it was found that although quite effective in decreasing thermal decomposition, 45% (mass/mass) more *t*-decalin was consumed as compared with THQ. Indeed, *t*-decalin was striking in that it was the hydrogen donor that was the most readily consumed in that study.²⁷ The decomposition products resulting

from the *t*-decalin consumption were highly stable C2 to C4 alkyl aromatic compounds, the presence of which gave added stability to the surrogate even at elevated temperatures.

We also note that the addition of these additives lowers the temperatures of the distillation curves by a few degrees. Adding 1% of any of the three additives lowers the temperatures along the curves by approximately 3 °C, whereas adding 3% lowers

the temperatures by 5–6 °C. This is expected because each of the additives has a much lower normal boiling temperature than that of a typical biodiesel fuel. We also note that the distillation curves take on a more sigmoidal shape due to the influence of a lighter component being present at a relatively high concentration. We have noted this kind of behavior develop upon the addition of other additives such as petroleum diesel fuel oxygenates.²¹

Stabilized Biodiesel Fuel-Composition Channel Information. Whereas the examination of the distillation curves is instructive and valuable for many design purposes, the composition channel of the ADC can provide even greater understanding and information content. One can sample and examine the individual fractions as they emerge from the condenser, as discussed in the introduction. Following the analytical procedure described in the experimental section, selected fractions were sampled and prepared for analysis by dissolving 7 L aliquots in autosampler vials with *n*-hexane as a solvent. The vials were weighed before and after introduction of the distillate fraction aliquot. The analyses were done by gas chromatography with mass spectrometric detection (30 m capillary column with a 0.1 mm coating of 50% cyanopropyl/50% dimethylpolysiloxane, split/splitless injector set with a 50 to 1 split ratio, injector operated at of 325 °C and a constant head pressure of 10 psig). For each of the mixtures of B100 with hydrogen donor additives, we sampled and analyzed the distillate at the first drop (at a distillate volume fraction of 0.025) and then at fractions of 0.2 to 0.6. The heavy residue left in the distillation flask was also sampled and analyzed. The analyses were standardized by preparing three mixtures of the pure hydrogen donors in *n*-tetradecane as external standards. These standards were prepared gravimetrically at concentrations of 1, 0.1, and 0.01% (mass/mass), and the response was found to be linear with correlation coefficients typically in the range of 0.998. The standards were injected immediately prior to the distillate fraction samples. In previous work on B100, we analyzed for the individual FAME constituents of biodiesel fuel; in this work we focus only on the hydrogen donor additive and the reaction products expected from them. The typical combined uncertainty in each analysis is 3%.

In Figure 5, we present a summary of the analyses as histograms showing the concentration on a mass basis. First to be noted is the differences in hydrogen donor concentration between the 1 and 3% starting mixtures. As expected, the mixtures with the higher starting concentrations always show a much higher concentration of hydrogen donor in the distillate fractions, as expected. The concentration ratio is not 1:3, however, because distillation is not the only process that is occurring. The hydrogen donor is also being consumed reactively, as we mentioned above and has been discussed in previous studies. Considering the difference between the 0.025 distillate fractions for THQ, we note a concentration ratio of approximately 2.7, relatively close to the starting ratio. Considering the same ratio for *t*-decalin, we note a lower ratio of 1.9. This is consistent with the observation in the previous section that *t*-decalin is consumed to a greater degree than THQ. The mixtures with 3% additive show that the additive is more

persistent; the concentrations are higher in later distillate fractions that are observed with the 1% solutions. In general, the persistence is in the expected order with respect to boiling temperature: THQ > tetralin > *t*-decalin.

We note that, for THQ, the hydrogen donor with the highest boiling temperature, detectable THQ persists into the 0.6 distillate fraction for both the 1 and 3% mixtures. For tetralin, the fluid with the next highest boiling temperature, the additive is observed to persist into the 0.4 distillate fraction. On the other hand, *t*-decalin, the hydrogen donor with the lowest boiling temperature, is not observed beyond the first distillate fraction at 0.025; it appears to be depleted before the 0.2 distillate fraction emerges. This is consistent with our distillation curve temperature dispersion measurement; the value of *t*-decalin as a hydrogen donor additive is observed to be very effective early in the distillation and less effective later in the distillation.

The expected decomposition products of the hydrogen donor additives are C2 to C4 alkyl aromatic hydrocarbons. We noted in the analyses of distillate fractions that indeed such fluids do appear in an emergent suite of chromatographic peaks. There are peaks for toluene, the xylenes, ethylbenzene, and *x*-ethyl-*y*-methylbenzenes, especially in the 0.025 and 0.2 fractions. At present, the relative quantities of these products appears to be: ethylbenzene > toluene \approx xylenes > the *x*-ethyl-*y*-methylbenzenes. Work is ongoing to better characterize this emergent suite.

Conclusions

In this article, we have had a 2-fold purpose. First, we have demonstrated how the advanced distillation curve metrology can be extended to approximate the combined thermal and oxidative stability of sensitive fluids such as FAME-based biodiesel fuels. This has been done by quantifying the dispersion that one measures among successive curves. We have concluded that the standard deviation in temperature at each distillate fraction, averaged over the entire curve, can be used to describe the curve repeatability, and, by extension, the combined thermal/oxidative decomposition potential. We then used this parameter to assess the performance of three hydrogen donor molecules (1,2,3,4-tetrahydroquinoline (THQ), 1,2,3,4-tetrahydronaphthalene (tetralin), and *trans*-decahydronaphthalene (*t*-decalin)) as high-temperature stabilizing additives for biodiesel fuel. We found that indeed these three additives can stabilize biodiesel fuel at elevated temperatures, even at temperatures encountered in the distillation of these fuels at atmospheric pressure. As expected from other studies, THQ and *t*-decalin perform similarly and outperform tetralin in all tests. For 1% additive solutions, THQ performs best overall; however, *t*-decalin performs best early in the distillations, before it is consumed or distilled out. In the near future, we plan to incorporate a specific oxygen analysis into the ADC metrology to further characterize distillate fractions.

Acknowledgment. This work was performed while A.W. and A.N. were supported by Summer Undergraduate Research Fellowship (SURF) awards at NIST.

EF800740D